Original Article

METTL14 inhibits the proliferation, migration and invasion of prostate cancer cells by increasing m6A methylation of CDK4

Xuesong Zhong[1], Sixue Wang[1], Xiaoli Yang[1], Xi Yang[2], Linchang Zhou[1]^

[1]Department of Urology, People's Hospital of Chuxiong Yi Autonomous Prefecture, Chuxiong City, China; [2]Department of Reproductive, People's Hospital of Chuxiong Yi Autonomous Prefecture, Chuxiong City, China

Contributions: (I) Conception and design: X Zhong, S Wang, Xiaoli Yang, L Zhou; (II) Administrative support: L Zhou; (III) Provision of study materials or patients: L Zhou; (IV) Collection and assembly of data: X Zhong, S Wang, Xiaoli Yang, Xi Yang; (V) Data analysis and interpretation: X Zhong, L Zhou; (VI) Manuscript writing: All authors; (VII) Final approval of manuscript: All authors.

Correspondence to: Linchang Zhou, MS. Department of Urology, People's Hospital of Chuxiong Yi Autonomous Prefecture, No. 318, Lucheng South Road, Chuxiong City 675000, China. Email: zhoulinchang0320@163.com.

Background: Methyltransferase-like (METTL) plays an important role in various biological processes, but its role in prostate cancer (PCa) is still unclear. This study aimed to explore the mechanism by which methyltransferase-like 14 (METTL14) inhibits the physiological activity of PCa cells by increasing the N6-methyladenosine (m6A) modification of cyclin-dependent kinase 4 (CDK4).

Methods: Clinical samples were collected for bioinformatics analysis. A PCa mouse model was constructed. Cell counting kit-8 (CCK-8), flow cytometry, colony formation assays, scratch assays, Transwell assays, real-time quantitative polymerase chain reaction (RT-qPCR), immunofluorescence and western blotting were used to detect the corresponding indicators.

Results: METTL14 was found to be beneficial to inhibit the proliferation, invasion, and migration of PCa cells. When the m6A RNA increased, the half-life of CDK4 mRNA decreased after oe-METTL14 (overexpression of METTL14). Overexpression of CDK4 reversed the effect of oe-METTL14. Coimmunoprecipitation experiments revealed there were interactions between CDK4 and forkhead box M1 (FOXM1). Transfection of si-CDK4 was similar to transfection of oe-METTL14. After transfection with oe-FOXM1, the invasion and migration ability of cells increased, and cell apoptosis decreased. After transfection with si-FOXM1 alone, autophagy related 7 (ATG7) expression was significantly downregulated, and autophagy levels were reduced. The overexpression of ATG7 reversed the effect of si-FOXM1. The tumor volume and weight of the oe-METTL14 group mice were significantly reduced, and tumor proliferation was decreased in comparison to untreated tumor-bearing mice.

Conclusions: METTL14 inhibits the invasion and migration of PCa cells and induces cell apoptosis by inhibiting CDK4 stability and FOXM1/ATG7-mediated autophagy.

Keywords: Prostate cancer (PCa); methyltransferase-like 14 (METTL14); cyclin-dependent kinase 4 (CDK4); N6-methyladenosine methylation (m6A methylation); forkhead box M1 (FOXM1)

Submitted Dec 29, 2023. Accepted for publication May 16, 2024. Published online Jul 16, 2024.
doi: 10.21037/tau-23-682
View this article at: https://dx.doi.org/10.21037/tau-23-682

^ ORCID: 0009-0008-6650-8399.

Introduction

Prostate cancer (PCa) is one of the most common cancers in men and the second leading cause of cancer death in men (1). Although some new treatment strategies have been identified, the mortality rate of PCa patients remains high. In 2024, the incidence of PCa accounts for approximately 29% of all cancer cases (2,3). Hence, it is important to investigate the molecular pathogenesis of PCa and to locate its potential medical value.

It is well known that targeting cyclin-dependent kinases (CDKs) to block cancer cell proliferation can inhibit cancer progression (4). Cyclin-dependent kinase 4 (CDK4) is involved in the cell cycle transition from G1 to S phase and is associated with the proliferation of sensitive cancer cells (5), such as glioblastoma (6) and melanoma cells (7). Among them, CDK4/6 inhibition enhances oncolytic virus efficacy by potentiating tumor-selective cell killing (6). Furthermore, combined therapy with a CDK4/6 inhibitor and antimelanoma chemotherapeutic agents will be a reasonable strategy for future clinical trials (8). In recent years, selective inhibitors of CDK4 have been developed, and cancer treatment strategies targeting CDK4 have received increasing attention (9,10). Moreover, inhibition of the *CDK4* gene promotes G1 cell cycle arrest to block the growth of PCa (11,12). According to the above studies, CDK4 plays an important role in cancer, including PCa. Therefore, it is necessary to further study CDK4 and reveal its specific mechanism in PCa.

In cells, chemical modification of RNA is an effective way to regulate RNA function, and N6-methyladenosine (m6A) RNA modification accounts for the most abundant posttranscriptional RNA modification on eukaryotic RNAs (13). Moreover, m6A methylation is closely related to the physiological activities of various cancer cells, including urological tumors such as PCa (14), renal cell carcinoma (15), and bladder cancer (16). m6A is modified by methyltransferase-like 3 (METTL3), METTL14, and Wilms tumor 1-associated protein (WTAP) and removed by fat mass and obesity-associated protein (FTO) and alkB homolog 5 (ALKBH5) (17). In most tumors, METTL14, a tumor suppressor gene, inhibits the occurrence and development of tumors by functioning as an m6A methyltransferase (18). It is known that METTL14-mediated m6A modification suppresses gastric cancer progression (19). Moreover, METTL14 inhibits colorectal cancer metastasis by regulating m6A methylation of methyl CpG binding protein 2 (20). Chen *et al.* reported that METTL14 mediates the m6A modification of SOX4 mRNA to inhibit colorectal cancer metastasis (21). These studies suggest that METTL14 regulates tumor progression by modifying the protein and mRNA expression of regulatory genes through methylation. However, the mechanisms underlying METTL14 and m6A modifications in PCa progression remain unclear and require further exploration.

We hypothesize that METTL14 may influence the progression of PCa by regulating the m6A methylation of CDK4, and the underlying mechanism was investigated in this study, which may provide new insight and further research directions for the treatment of PCa. We present this article in accordance with the ARRIVE and MDAR reporting checklists (available at https://tau.amegroups.com/article/view/10.21037/tau-23-682/rc).

Highlight box

Key findings

- Methyltransferase-like 14 (METTL14) inhibits the invasion and migration of prostate cancer (PCa) cells and induces cell apoptosis by inhibiting cyclin-dependent kinase 4 (CDK4) stability and forkhead box M1/autophagy related 7 (FOXM1/ATG7)-mediated autophagy.

What is known and what is new?

- METTL14 plays an important role in various cancer processes, and N6-methyladenosine (m6A) RNA modification is the most abundant posttranscriptional RNA modification.
- METTL14 expression is downregulated in PCa clinical samples and PCa cells. Overexpression of METTL14 inhibits proliferation, invasion and autophagy in PCa cells. METTL14 regulates m6A methylation to inhibit CDK4 stability. CDK4 regulates FOXM1/ATG7 to mitigate the malignant progression of PCa cells.

What is the implication, and what should change now?

- This study showed METTL14 inhibits the invasion and migration of PCa cells and induces cell apoptosis by inhibiting CDK4 stability and FOXM1/ATG7-induced autophagy, which provides a new theoretical basis for the treatment of PCa.

Methods

Clinical samples

Cancer tissue and paracancerous tissue were collected from patients with PCa (n=24, People's Hospital of Chuxiong Yi Autonomous Prefecture). Patients with other serious diseases or who started treatment within three months before admission were excluded. The study was approved

Table 1 Primer sequences

Gene	Primer	Sequence (5'-3')
METTL14	Forward	5'-GGCTGGCTCACAGTTGGAC-3'
	Reverse	5'-TCCACCTCCTCGGTCAGATT-3'
CDK4	Forward	5'-GGTGTATGGGGCCGTAGGA-3'
	Reverse	5'-AAAGCCACCTCACGAACTGT-3'
GAPDH	Forward	5'-GGAGTCCACTGGTGTCTTCA-3'
	Reverse	5'-GGGAACTGAGCAATTGGTGG-3'

METTL14, methyltransferase-like 14; *CDK4*, cyclin-dependent kinase 4; *GAPDH*, glyceraldehyde-3-phosphate dehydrogenase.

by the ethical committee of People's Hospital of Chuxiong Yi Autonomous Prefecture (No. 2021-023), and the participants provided written informed consent for inclusion in the study. The study was conducted in accordance with the Declaration of Helsinki (as revised in 2013).

Cell culture

Human PCa cells (PC3 and DU145) and the human prostate epithelial cell RWPE1 were purchased from Otwo Biotechnology Co., Ltd. (Shenzhen, China). All cells were grown and passaged in RPMI 1640 medium (Gibco, USA) supplemented with 1% penicillin and streptomycin (Sigma-Aldrich, USA) and 10% fetal bovine serum (FBS; Gibco, USA). All cells were incubated in an incubator with 5% CO_2 at 37 ℃.

Cell transfection

The pcDNA3.1(+)-METTL14 plasmid [oe-METTL14 (overexpression of METTL14)], pcDNA3.1(+)-CDK4 plasmid [oe-CDK4 (overexpression of CDK4)], pcDNA3.1(+)-FOXM1 plasmid (oe-FOXM1) and pcDNA3.1(+) plasmid [negative control-overexpression (NC-oe)] were designed and synthesized by GenePharma Biotechnology (Shanghai, China). Small interfering RNAs (siRNAs), including si-negative control (si-NC), si-FOXM1 and si-CDK4, were designed and synthesized by Sangon Biotechnology (Shanghai, China). The plasmids were transfected with Lipofectamine 3000 reagent (Invitrogen, CA, USA). The transfection efficiency was measured by real-time quantitative polymerase chain reaction (RT-qPCR) and western blotting, and subsequent experiments were carried out.

Experimental animals

In this study, male BALB/C mice (4–5 weeks old, 17–18 g) were selected as the experimental animals. The mice were fed for 2 weeks under specific pathogen-free (SPF) conditions at a temperature of 22–26 ℃, relative humidity of 52–58%, and a light/dark cycle of 12 h/12 h, after which the follow-up experiment was conducted. The mice were randomly divided into two groups (n=5). DU145 cells were injected into mice at a density of 5×10^6/mL (100 μL) to construct a mouse model of PCa (NC). For the oe-METTL14 group, PC cells transfected with oe-METTL14 were injected subcutaneously into the mice, and oe-METTL14 (10 ng) was injected into the mice via the caudal vein every 5 days. The mice were euthanized after 30 days, and the tumors were collected. Experiments were performed under a project license (No. ZQSW/LL23002_231108) granted by the Ethics Committee of People's Hospital of Chuxiong Yi Autonomous Prefecture, in compliance with institutional guidelines of People's Hospital of Chuxiong Yi Autonomous Prefecture for the care and use of animals. A protocol was prepared before the study without registration.

RT-qPCR

Total RNA was extracted from cells using TRIzol reagent (Invitrogen) and reverse-transcribed into single-stranded complementary DNA (cDNA) using the Prime Script™ RT kit with gDNA Eraser (Takara, China). RT-qPCR was performed using SYBR Green mix (Life Technologies, USA) according to the manufacturer's instructions. Glyceraldehyde-3-phosphate dehydrogenase (GAPDH) was used as an internal control. The $2^{-\Delta\Delta CT}$ method was used to calculate the relative gene expression, which was subsequently normalized. The primer sequences are detailed in *Table 1*.

RNA stability assay

Cells were treated with 5 μg/mL actinomycin D (Sigma-Aldrich, USA) according to the time course, and CDK4 mRNA expression was determined by RT-qPCR. The half-life (t1/2) of the CDK4 mRNA was calculated and normalized against that of GAPDH.

Western blots

Total protein from each group was extracted with RIPA buffer (Sigma-Aldrich). Then, the protein concentration

was determined according to the instructions of the bicinchoninic acid (BCA) detection kit (Thermo Scientific, USA). Total protein was separated by sodium dodecyl sulfate polyacrylamide gel electrophoresis (SDS-PAGE). The separated proteins were transferred to a polyvinylidene fluoride (PVDF) membrane (Millipore, USA). Then, the membranes were incubated with primary antibodies against METTL14 (1:1,000, ab309096), Bax (1:1,000, ab32503), Cleaved-caspase 3 (1:500, ab32042), Bcl-2 (1:1,000, ab182858) and LC3B II/I (1:2,000, ab192890) overnight at 4 ℃. Beclin1 (1:2,000, ab207612), p62 (1:10,000, ab109012), CDK4 (1:1,000, ab108357), FOXM1 (1:1,000, ab207298) and autophagy related 7 (ATG7) (1:10,000, ab133528) were identified. The membrane was incubated with a secondary antibody (1:4,000, ab97051, Abcam, UK) at room temperature for 1 h, and protein bands were visualized with an enhanced chemiluminescence (ECL) kit (Millipore). Finally, ImageJ software was used to conduct semiquantitative analysis of the bands.

Detection of cell viability

Cell viability was assessed with a cell counting kit-8 (CCK-8) kit (Beyotime, China). The cells (5×10^3) were seeded in 96-well plates and incubated at 37 ℃ and 5% CO_2 for 24 h. CCK-8 solution was added, and the culture was continued for 2 h. The 96-well plate was then placed on a microplate reader, and the absorbance was read at 450 nm.

Colony formation experiment

Five hundred cells were seeded in 35 mm culture dishes for 10 days. Colonies were counted in each well after staining with 0.1% crystal violet for 10 min.

Scratch test

The cells were seeded into 6-well plates at 1×10^5 cells/well. When the cells reached 100% confluence, a 1-mL spearhead was used to make scratches, the scratched cells were washed with phosphate buffer saline (PBS), and serum-free medium was added. The samples were cultured at 37 ℃ and 5% CO_2 and analyzed by microscopy at 0 and 24 h.

Transwell

The cells were digested with trypsin and made into a cell suspension with serum-free medium, and the cell density was adjusted to 1×10^5/mL. Two hundred microlitres of cell suspension was added to the upper chamber, 250 μL of culture medium containing 10% FBS was added to the lower chamber, and the cells were cultured in a 5% CO_2 incubator at 37 ℃ for 24 h. At the end of the culture, the chamber was removed and washed twice with PBS, and then the Matrigel and the upper layer of uninvaded cells were wiped off with a cotton swab, fixed with 4% paraformaldehyde at room temperature for 15 min, and then removed and dried upside down. After staining with 1% crystal violet for 20 min, the cells were washed twice with PBS, and after drying, they were photographed and counted.

Flow cytometry

After the cells from each treatment group were collected, they were washed with PBS three times, and the cells were subsequently resuspended in 100 μL of buffer. The cells were incubated with 5 μL of Annexin V-fluorescein isothiocyanate (FITC) and 5 μL of propidium iodide (PI) (BD Biosciences, USA) for 10 min at 4 ℃. Finally, after the addition of termination buffer, flow cytometry was performed to determine the percentage of apoptotic cells.

Quantification of m6A

Total RNA was isolated using TRIzol reagent (Invitrogen). An m6A RNA methylation quantification kit (ab185912; Abcam) was used to measure the m6A content in the total RNA. Two hundred nanograms of RNA was used to coat the assay wells. An RNA m6A quantification assay was performed following the manufacturer's protocol. The m6A content was quantified by measuring the absorbance at a wavelength of 450 nm.

Dot blot test

A dot-blot assay was performed as described previously. Extracted RNA was diluted 2-fold with PBS, denatured by heating at 72 ℃ for 5 min, chilled on ice immediately, and then transferred onto a nitrocellulose membrane (Amersham, GE Healthcare, USA). Then, the membrane was ultraviolet (UV) cross-linked, blocked, and incubated with a m6A-specific antibody (1:5,000, Abcam).

Coimmunoprecipitation experiment

The cells were collected and lysed for 15 min on ice with a

mixture of protease inhibitors (Beyotime) in hypotonic lysis buffer. The cell lysates were centrifuged at 12,000 rpm for 10 min at 4 ℃. A small amount of lysate was removed for western blot analysis, 1 μg of the corresponding antibody was added, and the sample was incubated overnight at 4 ℃ with slow shaking. Cell lysates containing 10 μL of protein A agarose beads and antibodies were incubated overnight at 4 ℃. The beads were collected by centrifugation and washed 3 times with lysis buffer. Protein elution was followed by immunoblot analysis.

Detection of autophagy

The level of autophagy was detected by staining with a monodansylcadaverine (MDC) probe (Sigma, St. Louis, MO, USA). The cells were observed and photographed under a fluorescence microscope.

Immunohistochemical staining

Human or mouse tumor tissues were removed and washed with PBS to prepare paraffin sections. The sections were subjected to routine dewaxing followed by immunoreaction. Primary antibodies against METTL14 (1:1,000, ab220030) and ki-67 (1:250, ab15580) were added successively, and the membranes were incubated with secondary antibodies (1:1,000, Abcam). The sections were stained with 3,3'-diaminobenzidine (DAB) after the excess PBS was removed, and then the sections were sealed for observation and analysis.

Statistical analysis

GraphPad Prism 7.0 software was used to analyze and prepare graphs of the experimental data, and the means ± standard deviations (SDs) were shown in this study. For the statistical comparison, Student's *t*-test was used when there were only two groups with differences between groups. Moreover, analysis of variance (ANOVA) was used when the experimental design included more than two groups. $P<0.05$ indicated statistical significance.

Results

METTL14 expression is downregulated in PCa clinical samples and cell lines

Bioinformatics analysis revealed that among the differentially expressed genes, the level of METTL14 in PCa clearly decreased (*Figure 1A*). METTL14 expression was evaluated by RT-qPCR, and METTL14 expression was clearly lower in PCa tissue than in paracancerous tissue (control) (*Figure 1B*). Immunohistochemical staining revealed that METTL14 was expressed at low levels in the PCa group (*Figure 1C*). In addition, compared to that in normal human prostate epithelial cells (RWPE1), METTL14 was downregulated in human PCa cells (PC3 and DU145) (*Figure 1D*).

Oe-METTL14 inhibits proliferation, invasion and autophagy in PC3 and DU145 cells

Oe-METTL14 was transfected into PC3 and DU145 cells, and RT-qPCR confirmed successful transfection of METTL14 (*Figure 2A*). After transfection with oe-METTL14, cell activity was significantly reduced compared to that in the NC group (*Figure 2B*). Moreover, compared to that in the NC group, cell colony formation in the oe-METTL14 group was significantly reduced (*Figure 2C*). The results of flow cytometry analysis showed that the apoptosis rate of cells significantly increased after transfection with oe-METTL14 (*Figure 2D*). Further detection of the expression of apoptosis-related proteins revealed that the expression of Bax and C-caspase 3 was significantly upregulated in the oe-METTL14 group, while the expression of Bcl-2 was significantly downregulated (*Figure 2E*). Compared with that in the NC group, METTL14 overexpression resulted in a decreased migration rate and decreased invasion ability (*Figure 2F-2G*). Further detection of the expression of autophagy-related proteins revealed that the expression of LC3B II/I and Beclin1 was significantly downregulated in oe-METTL14 group cells, while the expression of p62 was significantly upregulated (*Figure 2H*). The above results indicate that METTL14 inhibits proliferation, invasion and autophagy in PC3 and DU145 cells.

METTL14 regulates m6A methylation to inhibit CDK4 stability

METTL14 can regulate the expression of target genes through m6A methylation, thereby regulating tumor progression. Previous studies have shown that inhibiting the *CDK4* gene promotes G1 cell cycle arrest to block the growth of PCa (5). Next, we investigated the effect of METTL14, a m6A methyltransferase, on the stability of CDK4 mRNA. First, the m6A content significantly increased in comparison to that in the NC group after transfection with oe-METTL14 (*Figure 3A*), and the same results were further

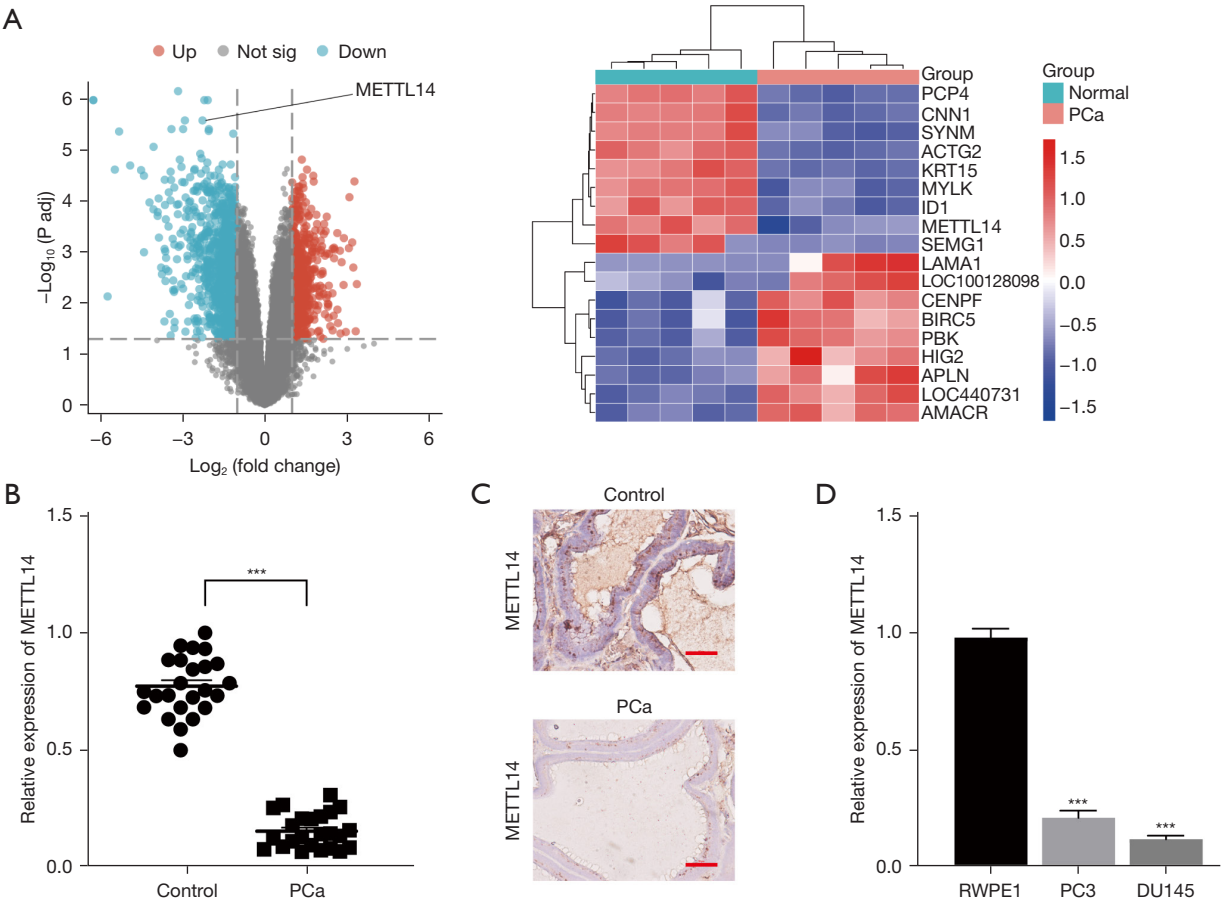

Figure 1 METTL14 expression is downregulated in PCa clinical samples and cell lines (n=3). (A) Bioinformatics analysis of METTL14. (B) METTL14 was detected by RT-qPCR in paracancerous tissue (control) and PCa tissue (n=24). (C) METTL14 was observed by immunohistochemistry (scale bar =50 μm). (D) METTL14 was detected by RT-qPCR in RWPE1, PC3, and DU145 cells. PC3 and DU145: human prostate cancer cells; RWPE1, human prostate epithelial cell. ***, P<0.001 compared with the control or RWPE1 group. METTL14, methyltransferase-like 14; PCa, prostate cancer; RT-qPCR, real-time quantitative polymerase chain reaction.

observed by dot blot assay (*Figure 3B*). Then, RT-qPCR was used to detect the expression of CDK4 mRNA in the two cell lines at different time points. The results showed that the half-life of CDK4 mRNA was significantly shortened in the oe-METTL14 group, and oe-METTL14 significantly reduced the stability of CDK4 mRNA in cells (*Figure 3C*). Moreover, western blot analysis revealed that METTL14 inhibited the expression of CDK4 (*Figure 3D*).

METTL14 regulates CDK4 to mitigate the malignant progression of PCa cells

Encouraged by the above results, we continued to investigate whether METTL14 affects the malignant progression of PCa cells by regulating CDK4. Oe-CDK4 was transfected into PC3 and DU145 cells, and western blots analysis confirmed the successful transfection of CDK4 (*Figure 4A*). Transfection of oe-METTL14 markedly reduced the proliferative viability of cells, while transfection of oe-CDK4 reversed the effect of oe-METTL14 (*Figure 4B*). Moreover, compared to that in the oe-METTL14 group, cell colony formation in the oe-METTL14 + oe-CDK4 group was significantly elevated (*Figure 4C*). Moreover, the percentage of apoptotic cells significantly increased after simultaneous transfection with oe-METTL14 and oe-CDK4 (*Figure 4D*). The expression of Bax and C-caspase 3 was significantly downregulated in the oe-METTL14 + oe-CDK4 group, while the expression of Bcl-2 was significantly upregulated (*Figure 4E*). Compared with those in the oe-METTL14 group, METTL14 and CDK4 overexpression resulted in an increased migration rate

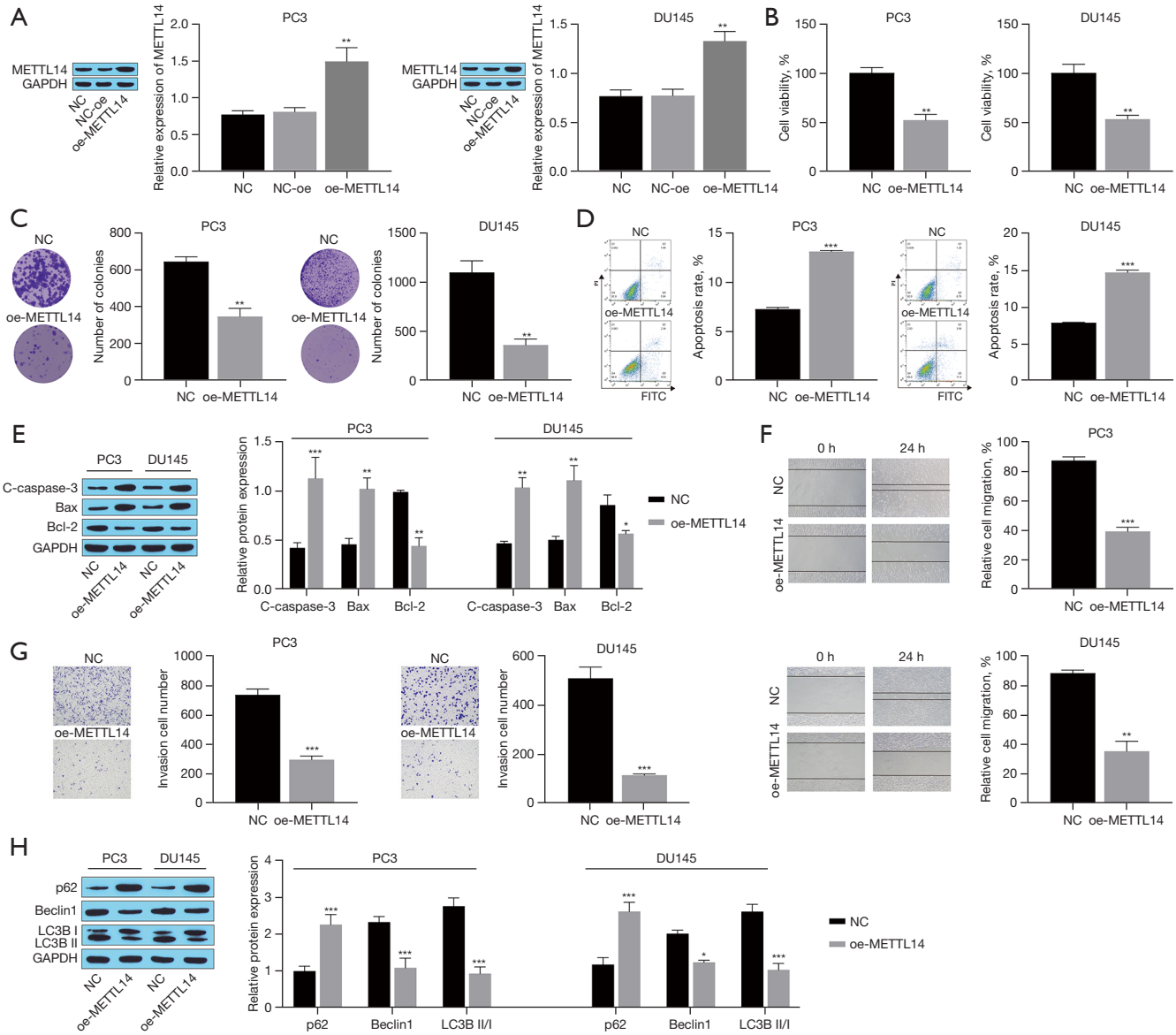

Figure 2 Oe-METTL14 inhibits proliferation, invasion and autophagy in PC3 and DU145 cells (n=3). (A) METTL14 expression was measured by western blotting. (B) Cell viability was tested by a CCK-8 kit. (C) Cell colony formation was detected by a colony formation assay (crystal violet staining, ×1). (D) Cell apoptosis was determined by flow cytometry. (E) Bax, Bcl-2 and cleaved caspase 3 were detected by western blotting. (F) The migration ability of cells was tested by a scratch test (×100). (G) The invasion ability of cells was measured by Transwell assays (crystal violet staining, ×100). (H) LC3B, p62 and Beclin1 were detected by western blotting. *, P<0.05, **, P<0.01, ***, P<0.001 compared with the NC-oe group or NC group. NC indicates untreated PC3 or DU145 cells. METTL14, methyltransferase-like 14; GAPDH, glyceraldehyde-3-phosphate dehydrogenase; oe-METTL14, overexpression of METTL14; FITC, fluorescein isothiocyanate; PI, propidium iodide; CCK-8, cell counting kit-8.

and increased invasive ability, as shown by the Transwell assay and scratch experiments (*Figure 4F,4G*). The above results indicate that METTL14 inhibits proliferation and invasion by regulating CDK4 in PC3 and DU145 cells.

Knocking down CDK4 attenuates the malignant progression of PCa cells through FOXM1

The transcription factor forkhead box M1 (FOXM1)

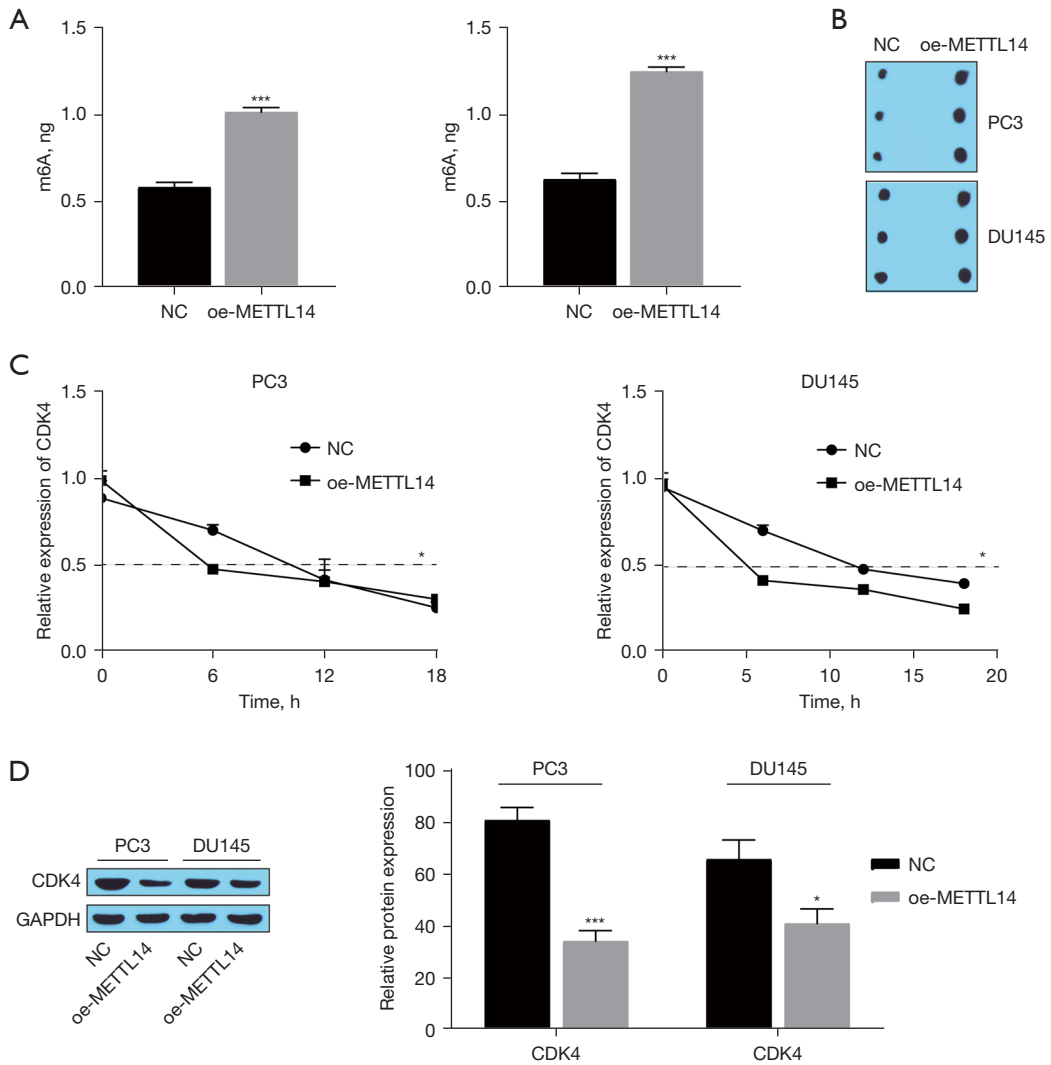

Figure 3 Oe-METTL14 inhibits proliferation, invasion and autophagy in PC3 and DU145 cells (n=3). (A) The m6A content was quantified with a m6A quantification kit. (B) Analysis of N6-methyladenosine RNA modification levels by dot blotting. (C) The stability of CDK4 RNA was detected by RT-qPCR. (D) CDK4 was detected by western blotting. *, P<0.05, ***, P<0.001 compared with the NC group. NC indicates untreated PC3 or DU145 cells. oe-METTL14, overexpression of methyltransferase-like 14; m6A, N6-methyladenosine; CDK4, cyclin-dependent kinase 4; GAPDH, glyceraldehyde-3-phosphate dehydrogenase; RT-qPCR, real-time quantitative polymerase chain reaction.

is a key factor in cell cycle regulation and is crucial for the progression of cell mitosis and chromosome stability (22). The direct binding relationship between CDK4 and FOXM1 in the two cell lines was confirmed through coimmunoprecipitation experiments (*Figure 5A*). Subsequently, si-CDK4 and oe-FOXM1 were transfected into two PCa cell lines, and western blots showed successful transfection of si-CDK4 and oe-FOXM1 (*Figure 5B,5C*). Transfection of si-CDK4 significantly reduced the proliferative viability of cells, while transfection of oe-FOXM1 reversed the effect of si-CDK4 (*Figure 5D*). Moreover, cell colony formation in the si-CDK4 group was significantly decreased in comparison to that in the NC group, but cell colony formation was markedly increased after transfection of oe-FOXM1 compared to that in the si-CDK4 group (*Figure 5E*). Compared with that of the NC group, the apoptosis rate of the si-CDK4 group was significantly greater, while the apoptosis rate decreased after transfection with oe-FOXM1 (*Figure 5F*). Further detection of the expression of apoptosis-related proteins

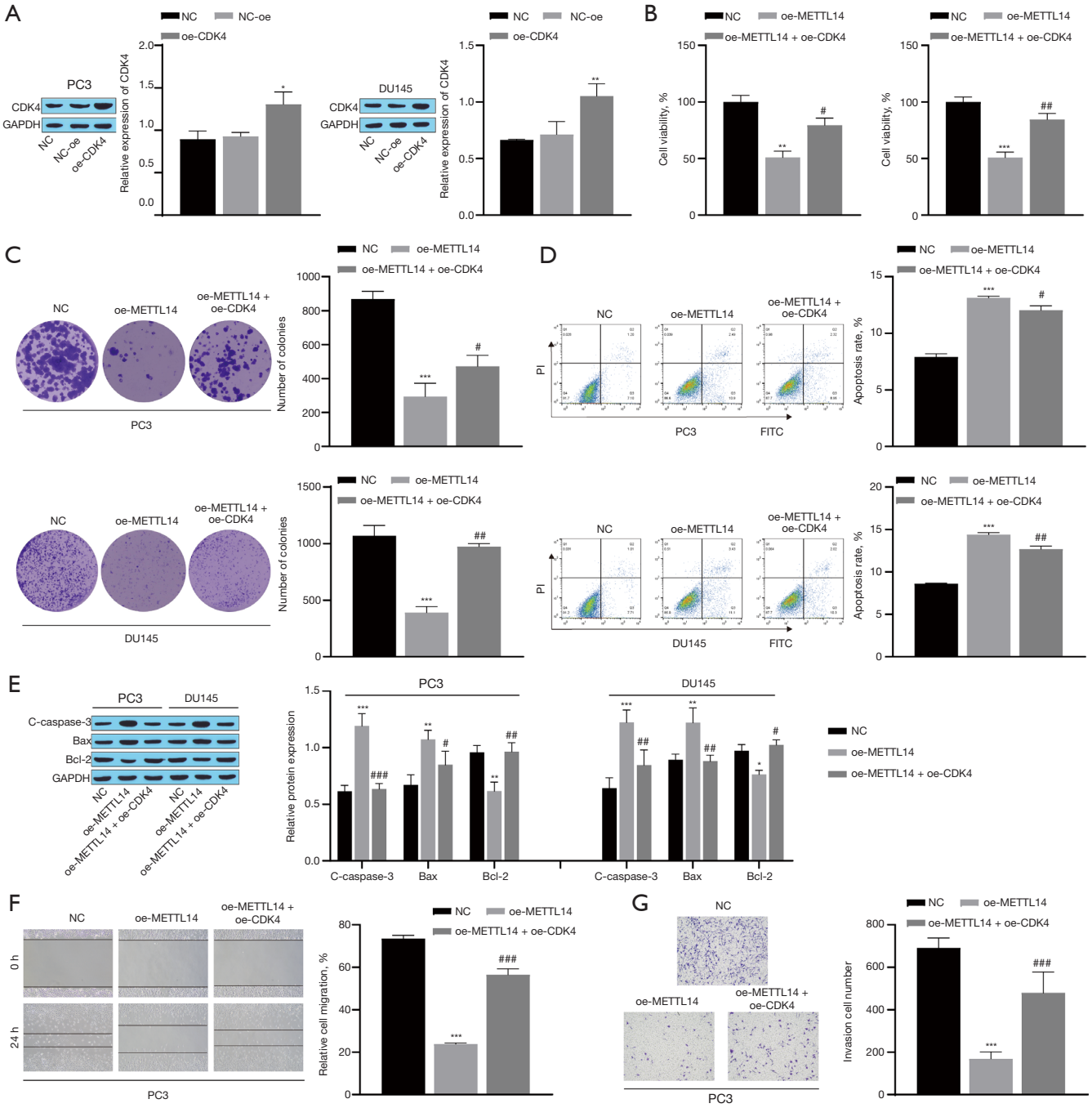

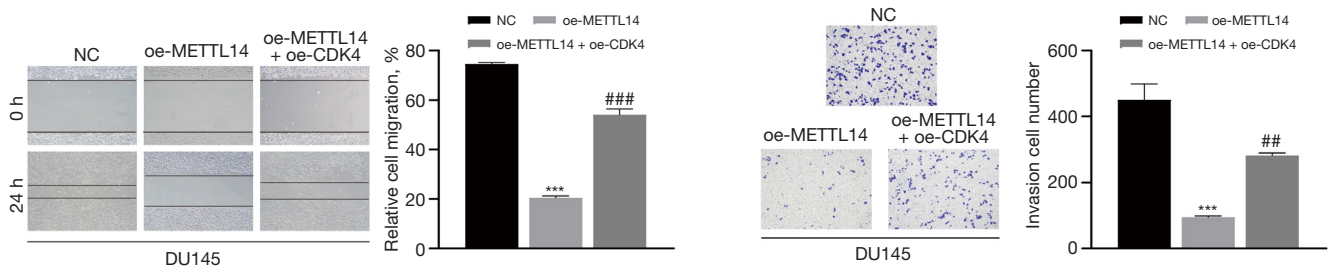

Figure 4 METTL14 regulates CDK4 to mitigate the malignant progression of PCa cells (n=3). (A) CDK4 was detected by western blotting. (B) Cell viability was tested by a CCK-8 kit. (C) Cell colony formation was detected by a colony formation assay (crystal violet staining, ×1). (D) Cell apoptosis was determined by flow cytometry. (E) Bax, Bcl-2 and cleaved caspase 3 were detected by western blotting. (F) The migration ability of cells was tested by a scratch test (×100). (G) The invasion ability of cells was measured by Transwell assays (crystal violet staining, ×100). *, P<0.05, **, P<0.01, ***, P<0.001 compared with the NC-oe or NC group; #, P<0.05, ##, P<0.01, ###, P<0.001 compared with the oe-METTL14 group. NC indicates untreated PC3 or DU145 cells. oe-CDK4, overexpression of cyclin-dependent kinase 4; CDK4, cyclin-dependent kinase 4; GAPDH, glyceraldehyde-3-phosphate dehydrogenase; oe-METTL14, overexpression of methyltransferase-like 14; FITC, fluorescein isothiocyanate; PI, propidium iodide; PCa, prostate cancer; CCK-8, cell counting kit-8.

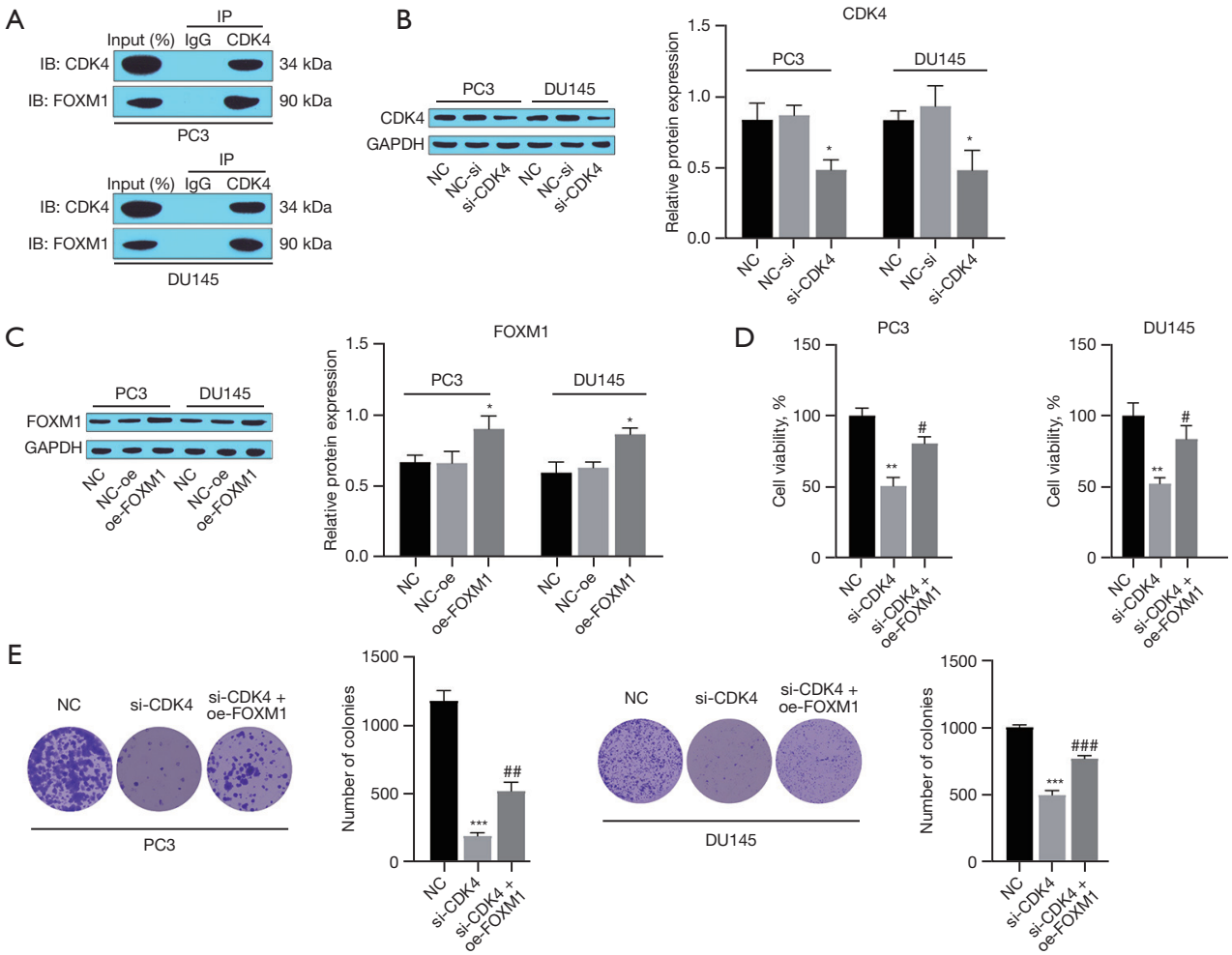

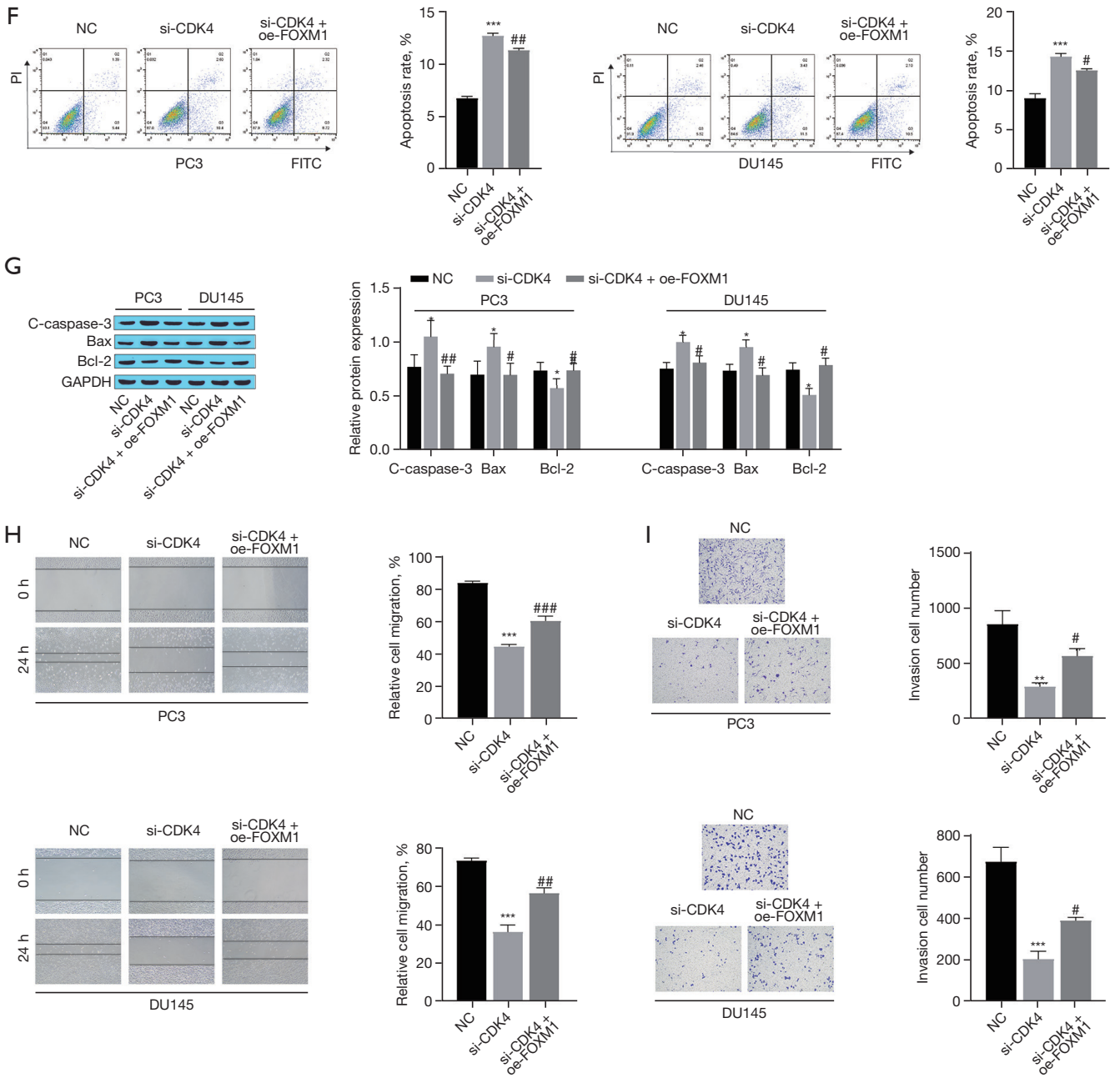

Figure 5 Knocking down CDK4 attenuates the malignant progression of PCa cells through FOXM1 (n=3). (A) The relationship between CDK4 and FOXM1 was detected by coimmunoprecipitation. (B) CDK4 was detected by western blotting. (C) FOXM1 was detected by western blotting. (D) Cell viability was tested by a CCK-8 kit. (E) Cell colony formation was detected by a colony formation assay (crystal violet staining, ×1). (F) Cell apoptosis was determined by flow cytometry. (G) Bax, Bcl-2 and cleaved caspase 3 were detected by western blotting. (H) The migration ability of cells was tested by a scratch test (×100). (I) The invasion ability of cells was measured by Transwell assays (crystal violet staining, ×100). *, P<0.05, **, P<0.01, ***, P<0.001 compared with the NC-si or NC group; #, P<0.05, ##, P<0.01, ###, P<0.001 compared with the si-CDK4 group. NC indicates untreated PC3 or DU145 cells. CDK4, cyclin-dependent kinase 4; FOXM1, forkhead box M1; IP, immunoprecipitation; GAPDH, glyceraldehyde-3-phosphate dehydrogenase; si-CDK4, small interfering-CDK4; oe-FOXM1, overexpression of forkhead box M1; FITC, fluorescein isothiocyanate; PI, propidium iodide; PCa, prostate cancer; CCK-8, cell counting kit-8.

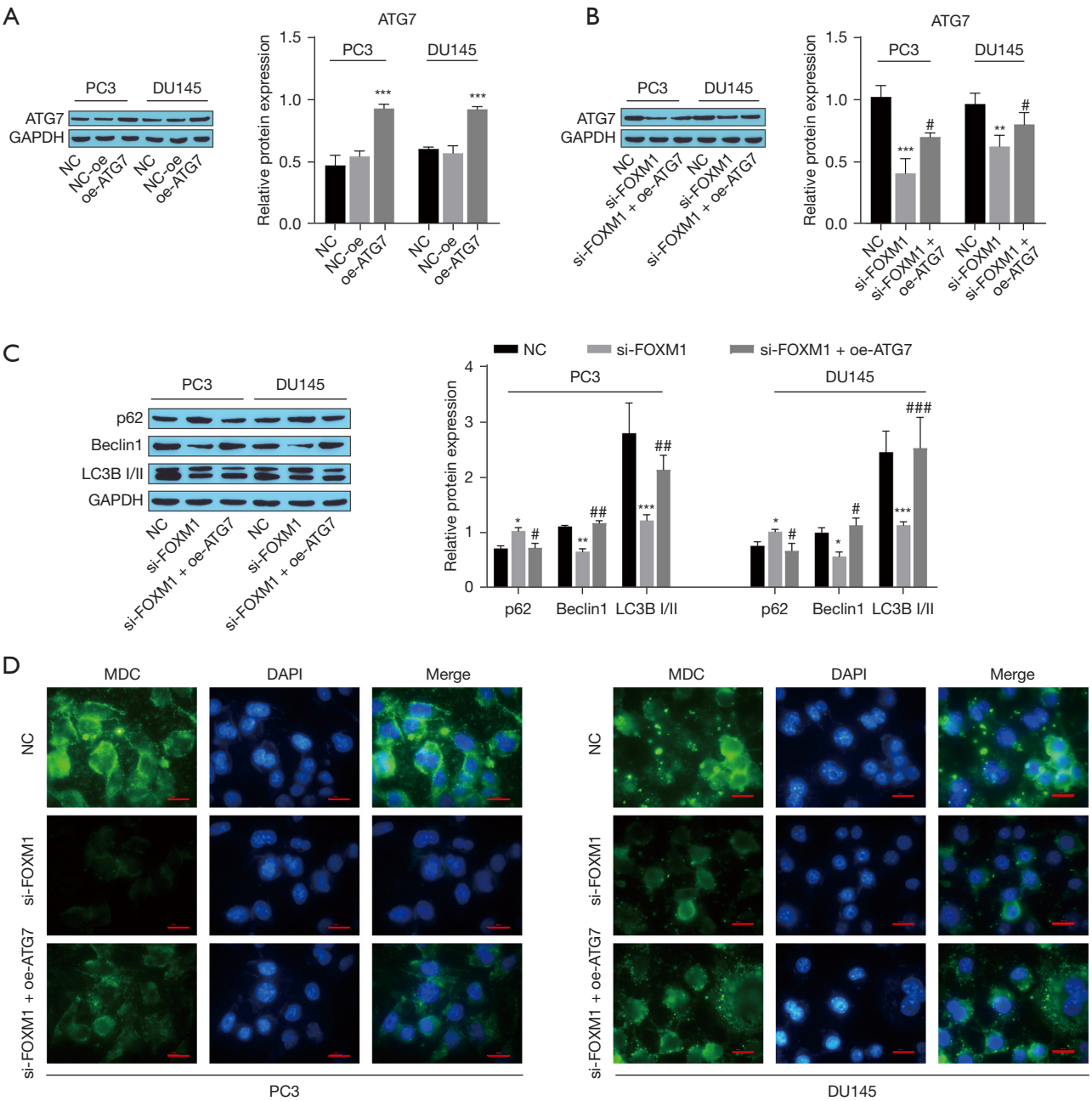

Figure 6 FOXM1 activates autophagy to mediate malignant progression in PCa cells by regulating ATG7 (n=3). (A,B) ATG7 was detected by western blotting. (C) LC3B, p62 and Beclin1 were detected by western blotting. (D) Autophagy was detected by MDC immunofluorescence (scale bar =10 μm). *, P<0.05, **, P<0.01, ***, P<0.001 compared with the NC-oe or NC group; #, P<0.05, ##, P<0.01; ###, P<0.001 compared with the si-FOXM1 group. NC indicates untreated PC3 or DU145 cells. ATG7, autophagy-related 7; oe-ATG7, overexpression of ATG7; GAPDH, glyceraldehyde-3-phosphate dehydrogenase; si-FOXM1, small interfering-forkhead box M1; MDC, monodansylcadaverine; DAPI, 4',6-diamidino-2-phenylindole; PCa, prostate cancer.

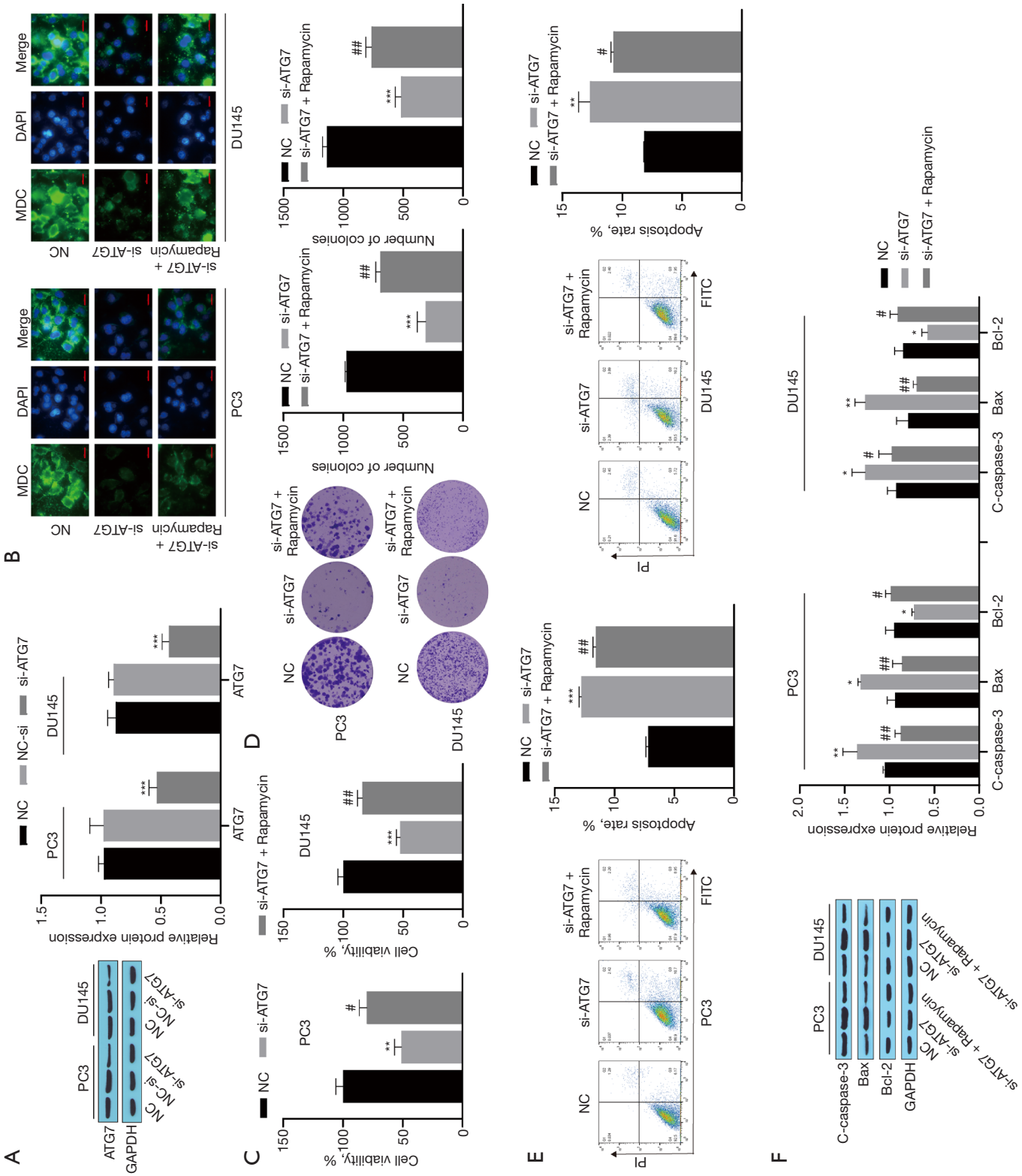

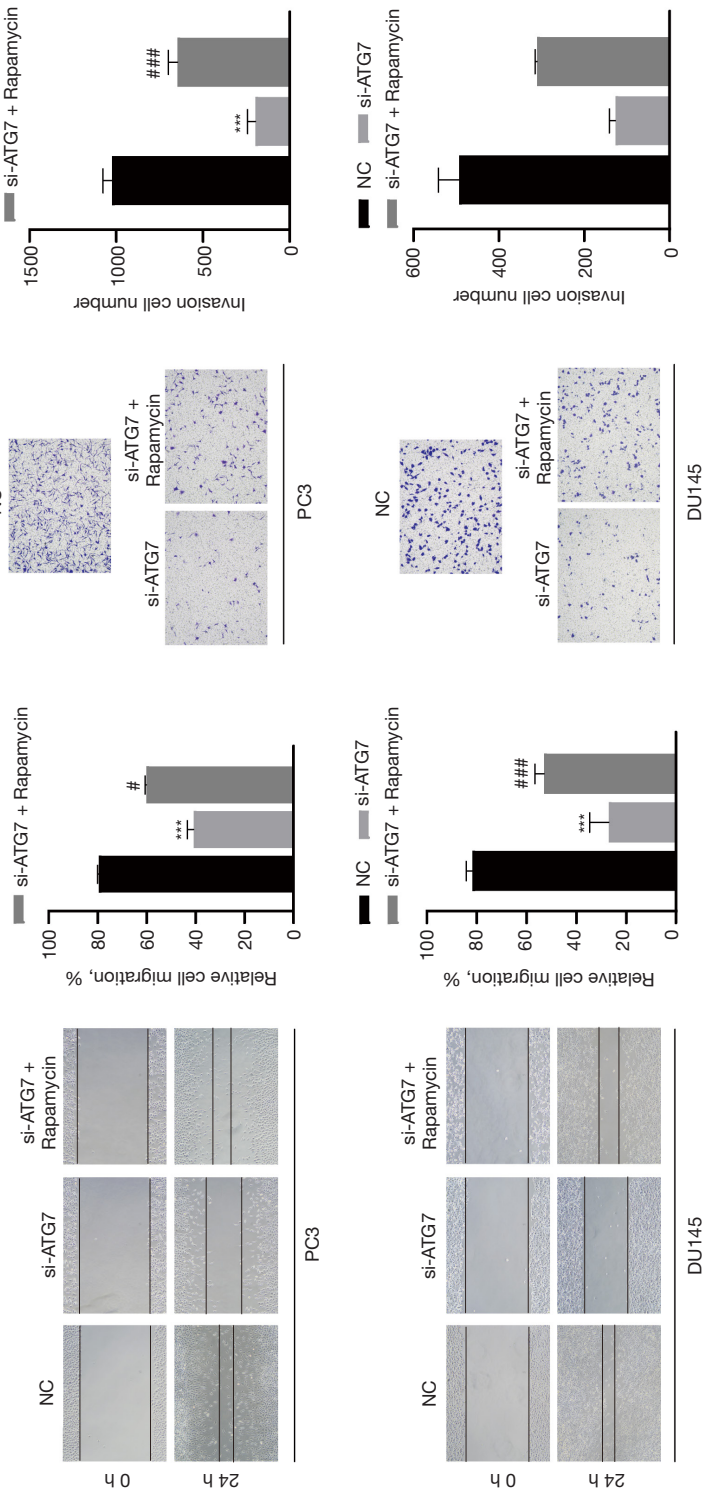

Figure 7 ATG7 regulates autophagy to inhibit the malignant progression of PCa cells (n=3). (A) ATG7 was detected by western blotting. (B) The autophagy level was observed by MDC immunofluorescence (scale bar =10 μm). (C) Cell viability was tested by a CCK-8 kit. (D) Cell colony formation was detected by a colony formation assay (crystal violet staining, ×1). (E) Cell apoptosis was determined by flow cytometry. (F) Bax, Bcl-2 and cleaved caspase 3 were detected by western blotting. (G) The migration ability of cells was tested by a scratch test (×100). (H) The invasion ability of cells was measured by Transwell assays (crystal violet staining, ×100). *, P<0.05, **, P<0.01, ***, P<0.001 compared with the NC-si or NC group; #, P<0.05, ##, P<0.01, ###, P<0.001, compared with the si-ATG7 group. NC indicates untreated PC3 or DU145 cells. ATG7, autophagy related 7; GAPDH, glyceraldehyde-3-phosphate dehydrogenase; si-ATG7, small interfering-ATG7; MDC, monodansylcadaverine; DAPI, 4',6-diamidino-2-phenylindole; FITC, fluorescein isothiocyanate; PI, propidium iodide; PCa, prostate cancer; CCK-8, cell counting kit-8.

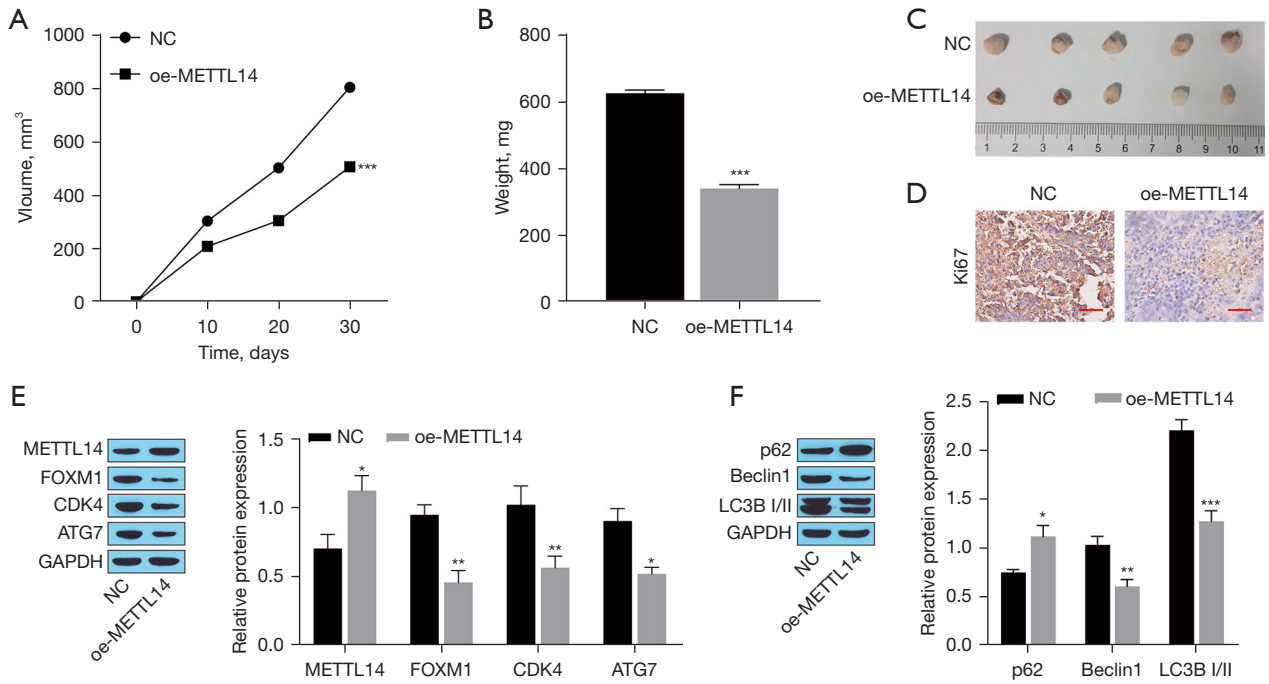

Figure 8 Overexpression of METTL14 inhibits the malignant progression of PCa *in vivo* (n=5). (A) Tumor volume was observed on Days 0, 10, 20, and 30. (B) Tumor weight was tested on Day 30. (C) Images of tumors on Day 30. (D) The expression of Ki-67 was detected by immunohistochemistry (scale bar =50 μm). (E) METTL14, FOXM1, CDK4 and ATG7 were detected by western blotting. (F) LC3B, p62 and Beclin1 were detected by western blotting. *, P<0.05, **, P<0.01, ***, P<0.001 compared with the NC group. NC indicates untreated tumor-bearing mice. oe-METTL14, overexpression of methyltransferase-like 14; FOXM1, forkhead box M1; CDK4, cyclin-dependent kinase 4; ATG7, autophagy related 7; GAPDH, glyceraldehyde-3-phosphate dehydrogenase; METTL14, methyltransferase-like 14; PCa, prostate cancer.

showed that after transfection with si-CDK4, the expression of Bax and C-caspase 3 was significantly upregulated, while the expression of Bcl-2 was significantly downregulated. However, transfection with oe-FOXM1 reversed the effect of si-CDK4 (*Figure 5G*). Transwell assays and scratch experiments revealed that the invasion and migration abilities of cells in the si-CDK4 group were significantly lower than those in the NC group, while the invasion and migration abilities of cells in the oe-FOXM1 group were significantly greater than those in the si-CDK4 group (*Figure 5H,5I*).

FOXM1 activates autophagy to mediate malignant progression in PCa cells by regulating ATG7

ATG7 is a core autophagy-related gene, and increased FOXM1 can activate ATG7, thereby promoting cellular autophagy (23). Oe-ATG7 was transfected into two PCa cell lines, and western blots analysis confirmed successful transfection (*Figure 6A*). Moreover, transfection of si-FOXM1 decreased the level of ATG7, and the effect of si-FOXM1 was reversed after transfection of oe-ATG7 (*Figure 6B*). Compared with those in the NC group, the expression of LC3B II/I and Beclin1 was significantly downregulated, but p62 had the opposite results, and the effect of si-FOXM1 was reversed after transfection with oe-ATG7 (*Figure 6C*). MDC is one of the most commonly used fluorescent probes for autophagy detection and can specifically label autophagosomes. The number of positive cells in the si-FOXM1 group was significantly reduced, indicating that the number of autophagosomes and the level of autophagy were reduced, while oe-ATG7 increased the number of positive cells (*Figure 6D*). These results indicate that FOXM1 activates autophagy in PCa cells by regulating ATG7.

ATG7 regulates autophagy to inhibit the malignant progression of PCa cells

si-ATG7 was transfected into two PCa cell lines, and an autophagy activator (rapamycin) was used. Western blots

indicated successful transfection of si-ATG7 (*Figure 7A*). There were significantly fewer MDC-positive cells in the si-ATG7 group, while rapamycin treatment reversed the effect of si-ATG7 (*Figure 7B*). Transfection of si-ATG7 significantly reduced the proliferative viability of cells, while rapamycin reversed the effect of si-ATG7 (*Figure 7C*). Moreover, cell colony formation in the si-ATG7 group was significantly lower than that in the NC group, but cell colony formation markedly increased after the addition of rapamycin (*Figure 7D*). Compared with that of the NC group, the apoptosis rate of the si-ATG7 group was significantly greater, while the apoptosis rate decreased after the addition of rapamycin (*Figure 7E*). Further detection of the expression of apoptosis-related proteins showed that after transfection with si-ATG7, the expression of Bax and C-caspase 3 was significantly upregulated, while the expression of Bcl-2 was significantly downregulated. However, rapamycin reversed the effect of si-ATG7 (*Figure 7F*). Transwell assays and scratch experiments revealed that the invasion and migration ability of cells in the si-ATG7 group were significantly lower than those in the NC group, while rapamycin promoted the invasion and migration ability of cells (*Figure 7G,7H*).

Oe-METTL14 inhibits the malignant progression of PCa in vivo

Mice were divided into the NC group and oe-METTL 14 group; the NC group included PCa model mice, and the oe-METTL14 group included PCa mice treated with METTL14. Compared to the NC group, the oe-METTL14 group showed a significant reduction in tumor volume and weight (*Figure 8A-8C*). Immunohistochemical staining was used to detect the expression of Ki-67 in tumor tissues, and the results showed that the expression of Ki-67 in tumor tissues of mice in the oe-METTL14 group was reduced compared to that in the NC group (*Figure 8D*). In addition, METTL1 expression was upregulated, and FOXM1, CDK4, and ATG7 expression was downregulated in mouse tumor tissue in the oe-METTL14 group (*Figure 8E*). The expression of p62 was significantly upregulated, while the expression of LC3B II/I and Beclin1 was significantly downregulated (*Figure 8F*). The above results indicate that METTL1 inhibits the malignant proliferation of PCa tumors by inhibiting CDK4/FOXM1/ATG7.

Discussion

RNA modification plays a crucial role in many biological functions, among which m6A is the most abundant RNA modification, and its abnormalities are related to regulating cancer progression (24). METTL14 is a core component of the m6A methyltransferase complex, and its induction of abnormal m6A levels is closely related to cancer progression (25). Therefore, studies on the biological function of METTL14 as a novel cancer diagnostic biomarker in human tumors have received increasing attention (18). Wu *et al.* reported that METTL14 expression was negatively correlated with the Gleason score in PCa (26). This finding suggested that METTL14 is involved in the progression of PCa, but the specific mechanism involved is not clear. Our current findings suggest that METTL14 is expressed at low levels in the tissues of PCa patients and PCa cell lines (PC3 and DU145). Oe-METTL14 inhibits the proliferation, invasion, and migration of PC3 and DU145 cells. Autophagy was significantly reduced in cells overexpressing METTL14. Second, oe-METTL14 resulted in a significant increase in the m6A content in cells. Our results are consistent with those of previous studies, further indicating that METTL14 participates in the proliferation, invasion, and migration of PCa by inducing changes in m6A levels.

Previous studies have confirmed that inhibiting the expression of the CDK4 gene can block the growth of PCa (9,10). In addition, research has confirmed that METTL14 regulates the protein and mRNA expression of genes through methylation, thereby regulating tumor progression (20). Therefore, we infer that METTL14 may regulate the stability of CDK4 mRNA and protein expression by inducing the m6A modification of CDK4 and may participate in the physiological process of PCa. In this study, after oe-METTL14, the m6A content of total RNA in cells significantly increased, and the half-life of CDK4 mRNA decreased, accompanied by downregulation of CDK4 protein expression. Overexpression of CDK4 promoted the proliferation, invasion, and migration of PC3 and DU145 cells. The above results indicate that in PC3 and DU145 cells, METTL14 can regulate the stability of CDK4 mRNA and CDK4 expression by mediating m6A methylation, affecting the cell cycle and thereby regulating the growth of PCa cells.

Similarly, FOXM1 is also a key factor in cell cycle regulation, mainly regulating the G2 transcription program, which is crucial for the progression of cell mitosis and chromosome stability (27). Furthermore, the data suggest that CDK4/6 initiates FOXM1 phosphorylation, which directly activates FOXM1 transcriptional function (28). In this study, immunoprecipitation experiments revealed an interaction between CDK4 and FOXM1. After knocking down CDK4,

the invasion and migration ability of cells decreased, and cell apoptosis increased. FOXM1 overexpression reversed the above results. These results suggest that knocking down CDK4 may alleviate the malignant progression of PCa cells by reducing the phosphorylation of FOXM1.

Autophagy is considered a clear self-digestion process used to degrade proteins and organelles in response to cellular stress, maintaining cellular homeostasis and promoting cell survival. ATG7 is a core autophagy-related gene involved in the formation of autophagosomes (29,30). One study suggested that ATG7 may be a functional target of FOXM1 during autophagy, ultimately confirming the relationship between FOXM1 and ATG7-dependent autophagy (23). Interestingly, FOXM1 knockdown downregulated the protein expression of ATG7 and inhibited autophagy in PCa cells. ATG7 overexpression reversed the inhibitory effect of si-FOXM1 on autophagy. This finding is similar to the results of Myojin *et al*., who reported that high expression of ATG7 promotes cellular autophagy and hepatoma carcinoma cell proliferation (31). In addition, knocking down ATG7 alone inhibited the autophagy of PCa cells, promoted their apoptosis, and inhibited their invasion and migration ability. The addition of the autophagy activator rapamycin reversed the effect of si-ATG7. The above results revealed that FOXM1 can regulate the autophagy level of PCa cells by regulating the expression of ATG7, thereby affecting the physiological processes of PCa cells.

Finally, the physiological effects of METTL14 were validated in tumor-bearing nude mice. The results showed that the tumor volume and weight of the oe-METTL14 group mice were significantly reduced, and the proliferation of cancer cells in the tumor tissue was weakened to some extent. In addition, western blot analysis revealed downregulation of FOXM1, CDK4, and ATG7 expression, significant upregulation of p62 expression, and significant downregulation of LC3B II/I and Beclin1 expression.

Conclusions

METTL14 inhibits the invasion and migration of PCa cells and induces cell apoptosis by inhibiting CDK4 stability and FOXM1/ATG7-induced autophagy, which provides a new theoretical basis for the treatment of PCa.

Acknowledgments

Funding: This study was supported by grants from the People's Hospital of Chuxiong Yi Autonomous Prefecture In-hospital Fund (grant number: 2021J23).

Footnote

Reporting Checklist: The authors have completed the ARRIVE and MDAR reporting checklists. Available at https://tau.amegroups.com/article/view/10.21037/tau-23-682/rc

Data Sharing Statement: Available at https://tau.amegroups.com/article/view/10.21037/tau-23-682/dss

Peer Review File: Available at https://tau.amegroups.com/article/view/10.21037/tau-23-682/prf

Conflicts of Interest: All authors have completed the ICMJE uniform disclosure form (available at https://tau.amegroups.com/article/view/10.21037/tau-23-682/coif). The authors have no conflicts of interest to declare.

Ethical Statement: The authors are accountable for all aspects of the work in ensuring that questions related to the accuracy or integrity of any part of the work are appropriately investigated and resolved. The study was approved by the ethical committee of People's Hospital of Chuxiong Yi Autonomous Prefecture (No. 2021-023), and the participants provided written informed consent for inclusion in the study. The study was conducted in accordance with the Declaration of Helsinki (as revised in 2013). Experiments were performed under a project license (No. ZQSW/LL23002_231108) granted by the Ethics Committee of People's Hospital of Chuxiong Yi Autonomous Prefecture, in compliance with institutional guidelines of People's Hospital of Chuxiong Yi Autonomous Prefecture for the care and use of animals.

References

1. Boehm BE, York ME, Petrovics G, et al. Biomarkers of

Aggressive Prostate Cancer at Diagnosis. Int J Mol Sci 2023;24:2185.
2. Tang F, Xu D, Wang S, et al. Chromatin profiles classify castration-resistant prostate cancers suggesting therapeutic targets. Science 2022;376:eabe1505.
3. Siegel RL, Giaquinto AN, Jemal A. Cancer statistics, 2024. CA Cancer J Clin 2024;74:12-49.
4. Zhang M, Zhang L, Hei R, et al. CDK inhibitors in cancer therapy, an overview of recent development. Am J Cancer Res 2021;11:1913-35.
5. Pandey P, Khan F, Upadhyay TK, et al. Deciphering the Immunomodulatory Role of Cyclin-Dependent Kinase 4/6 Inhibitors in the Tumor Microenvironment. Int J Mol Sci 2023;24:2236.
6. Xiao J, Liang J, Fan J, et al. CDK4/6 Inhibition Enhances Oncolytic Virus Efficacy by Potentiating Tumor-Selective Cell Killing and T-cell Activation in Refractory Glioblastoma. Cancer Res 2022;82:3359-74.
7. Garutti M, Targato G, Buriolla S, et al. CDK4/6 Inhibitors in Melanoma: A Comprehensive Review. Cells 2021;10:1334.
8. Lyu J, Miao Y, Yu F, et al. CDK4 and TERT amplification in head and neck mucosal melanoma. J Oral Pathol Med 2021;50:971-8.
9. Goel S, Bergholz JS, Zhao JJ. Targeting CDK4 and CDK6 in cancer. Nat Rev Cancer 2022;22:356-72.
10. Rugo HS, Lerebours F, Ciruelos E, et al. Alpelisib plus fulvestrant in PIK3CA-mutated, hormone receptor-positive advanced breast cancer after a CDK4/6 inhibitor (BYLieve): one cohort of a phase 2, multicentre, open-label, non-comparative study. Lancet Oncol 2021;22:489-98.
11. Wu C, Peng S, Pilié PG, et al. PARP and CDK4/6 Inhibitor Combination Therapy Induces Apoptosis and Suppresses Neuroendocrine Differentiation in Prostate Cancer. Mol Cancer Ther 2021;20:1680-91.
12. Guney Eskiler G, Deveci Ozkan A, Haciefendi A, et al. Mechanisms of abemaciclib, a CDK4/6 inhibitor, induced apoptotic cell death in prostate cancer cells in vitro. Transl Oncol 2022;15:101243.
13. Wen S, Wei Y, Zen C, et al. Long non-coding RNA NEAT1 promotes bone metastasis of prostate cancer through N6-methyladenosine. Mol Cancer 2020;19:171.
14. Ding L, Wang R, Zheng Q, et al. circPDE5A regulates prostate cancer metastasis via controlling WTAP-dependent N6-methyladenisine methylation of EIF3C mRNA. J Exp Clin Cancer Res 2022;41:187.
15. Ma T, Wang J, Liu X, et al. m6A Methylation Patterns and Tumor Microenvironment Infiltration Characterization in Clear-Cell Renal Cell Carcinoma. Front Genet 2022;13:864549.
16. Li F, Zheng Z, Chen W, et al. Regulation of cisplatin resistance in bladder cancer by epigenetic mechanisms. Drug Resist Updat 2023;68:100938.
17. Zhang B, Jiang H, Dong Z, et al. The critical roles of m6A modification in metabolic abnormality and cardiovascular diseases. Genes Dis 2021;8:746-58.
18. Guan Q, Lin H, Miao L, et al. Functions, mechanisms, and therapeutic implications of METTL14 in human cancer. J Hematol Oncol 2022;15:13.
19. Fan HN, Chen ZY, Chen XY, et al. METTL14-mediated m(6)A modification of circORC5 suppresses gastric cancer progression by regulating miR-30c-2-3p/AKT1S1 axis. Mol Cancer 2022;21:51.
20. Wang S, Gan M, Chen C, et al. Methyl CpG binding protein 2 promotes colorectal cancer metastasis by regulating N(6) -methyladenosine methylation through methyltransferase-like 14. Cancer Sci 2021;112:3243-54.
21. Chen X, Xu M, Xu X, et al. METTL14-mediated N6-methyladenosine modification of SOX4 mRNA inhibits tumor metastasis in colorectal cancer. Mol Cancer 2020;19:106.
22. Pan F, Chocarro S, Ramos M, et al. FOXM1 is critical for the fitness recovery of chromosomally unstable cells. Cell Death Dis 2023;14:430.
23. Lyu X, Zeng L, Shi J, et al. Essential role for STAT3/FOXM1/ATG7 signaling-dependent autophagy in resistance to Icotinib. J Exp Clin Cancer Res 2022;41:200.
24. An Y, Duan H. The role of m6A RNA methylation in cancer metabolism. Mol Cancer 2022;21:14.
25. Xie Q, Li Z, Luo X, et al. piRNA-14633 promotes cervical cancer cell malignancy in a METTL14-dependent m6A RNA methylation manner. J Transl Med 2022;20:51.
26. Wu Q, Xie X, Huang Y, et al. N6-methyladenosine RNA methylation regulators contribute to the progression of prostate cancer. J Cancer 2021;12:682-92.
27. Nandi I, Smith HW, Sanguin-Gendreau V, et al. Coordinated activation of c-Src and FOXM1 drives tumor cell proliferation and breast cancer progression. J Clin Invest 2023;133:e162324.
28. Anders L, Ke N, Hydbring P, et al. A systematic screen for CDK4/6 substrates links FOXM1 phosphorylation to senescence suppression in cancer cells. Cancer Cell 2011;20:620-34.
29. Collier JJ, Suomi F, Oláhová M, et al. Emerging roles of ATG7 in human health and disease. EMBO Mol Med

2021;13:e14824.
30. Wang X, Wu R, Liu Y, et al. m(6)A mRNA methylation controls autophagy and adipogenesis by targeting Atg5 and Atg7. Autophagy 2020;16:1221-35.
31. Myojin Y, Hikita H, Sugiyama M, et al. Hepatic Stellate Cells in Hepatocellular Carcinoma Promote Tumor Growth Via Growth Differentiation Factor 15 Production. Gastroenterology 2021;160:1741-1754.e16.

Cite this article as: Zhong X, Wang S, Yang X, Yang X, Zhou L. METTL14 inhibits the proliferation, migration and invasion of prostate cancer cells by increasing m6A methylation of CDK4. Transl Androl Urol 2024;13(7):1145-1163. doi: 10.21037/tau-23-682

